CERN-TH.4364/85

A COMPARISON OF πΔ INTERACTION MECHANISM WITH THE DOUBLE CHARGE EXCHANGE EXPERIMENTAL DATA ON SELF-CONJUGATE NUCLEI

C.R. Ching*), T.E.O. Ericson and T.H. Ho*)
CERN - Geneva

and

W.Q. Zhao+)

Freie Universität, Berlin

A B S T R A C T

It is shown that the πΔ interaction may be the dominant mechanism in the pion-induced double charge-exchange reaction (DCX) on self-conjugate nuclei. A comprehensive comparison of this hypothesis with the existing experiments is given. The agreement in both the excitation function and the angular distribution is encouraging. The $A^{-4/3}$ mass dependence relation is also obtained in a natural way.

---

*) On leave from Institute of Theoretical Physics, Academia Sinica, P.O. Box 2735, Beijing, China.

+) On leave from Institute of High Energy Physics, Academia Sinica, P.O. Box 918, Beijing, China.

CERN-TH.4364/85

February 1986

1. - INTRODUCTION

There is a general interest in studying the pion-induced double charge-exchange reactions (DCX) in nuclear physics. Recently, a relationship between the double β decay and DCX was emphasized using PCAC and the soft-pion approach[1]. This of course increases the importance of understanding the mechanism of DCX. The characteristic features of DCX in $\Delta I = 2$, $\Delta J = 0$ transitions on $I = 0$ target nuclei are the peaking of the excitation functions about the Δ_{33} resonance energy, the diffractive angular distribution behaviour and the $A^{-4/3}$ mass dependence. All these have not been explained satisfactorily[2),3)]. Several calculations for $^{16}O(\pi^+,\pi^-)\ ^{16}Ne(g.s.)$ have been performed, based upon the sequential charge exchange mechanism but with limited success[4)-6)]. Another suggestion is to explain all these features with a one-step mechanism such as[2),3),7)]

$$\pi^+ + N \longrightarrow \pi^- + \Delta \qquad (1)$$

However, as pointed out in one of our previous papers[8)], the one-step $N(\pi^+,\pi^-)\Delta$ mechanism is forbidden by a selection rule which has been shown in the theory of double β decay by Doi et al.[9)] and also by Haxton and Stephenson[10)]. In addition to this, a detailed calculation of Johnson et al.[11)] also shows that this mechanism contributes negligibly to DCX. Recently, Gilman et al.[12)] gave a numerical calculation, using the direct Δ_{33}-nucleus interaction process to account for the experimental results on $I = 0$ target nuclei. This calculation reproduces very well the angular and energy dependence behaviour, but the absolute magnitude and especially the A dependence of the excitation function are not correctly described. A closer analysis reveals that the DCX reactions on $I = 0$ target nuclei behave very similarly to the single charge-exchange (SCX) reactions between isobaric analogue states, but differ from that of the latter by three orders of magnitude[8)]. Therefore, since the SCX experimental results can be explained by one-step charge-exchange πN interaction, one would expect that some other one-step mechanism must be involved in explaining the DCX experiments. In Ref. 8), we have already suggested that the specific behaviour of DCX observed on $I = 0$ target nuclei may be explained by the following reaction mechanism:

$$\pi^+ + \Delta^0 \longrightarrow \pi^- + \Delta^{++} \qquad (2)$$

$$\pi^+ + \Delta^- \longrightarrow \pi^- + \Delta^+ , \qquad (3)$$

provided the Δ_{33} components exist in nuclei with a probability of a few per cent per nucleon. In this paper, we show that we can obtain a full description of the cross-section of DCX on I = 0 nuclei by combining the double charge-exchange of $\Delta^-(\Delta^\circ)(\pi^+,\pi^-)\Delta^+(\Delta^{++})$ and the eikonal-diffractive model[13),14)]. This procedure is simple and physically clear, and at the same time it is accurate enough for our purpose. The comparison of the theoretical results with all existing experimental data on I = 0 target nuclei shows that the agreement is quite encouraging.

The paper is organized as follows. Section 2 briefly gives a description of the eikonal Δ-dominance model. Section 3 shortly describes the calculation of DCX cross-section of $\Delta^-(\Delta^\circ)(\pi^+\ \pi^-)\Delta^+(\Delta^{++})$. Section 4 summarizes the experimental results on I = 0 self-conjugate target nuclei and compares them with the predictions of the eikonal Δ-dominance model. Section 5 discusses the relation and the internal consistency of DCX and SCX, and gives some predictions of the present model, which may be verified by future experiments.

An important question concerning the A dependence of the total number of Δ_{33} isobars inside the nucleus, which is crucial for the eikonal Δ-dominant model, is discussed in Section 6. Finally, Section 7 recapitulates the main conclusions obtained in this paper.

2. - THE EIKONAL Δ DOMINANCE MODEL AND THE DOUBLE CHARGE-EXCHANGE REACTION

According to our theoretical model, the mechanism of the double charge-exchange (DCX) reaction on nuclei for the $J^P = 0^+ \to 0^+$ transitions is mainly a single-step process in which the double charge exchange occurs on a Δ_{33} isobar inside the nucleus [Eqs. (2) and (3)]. The physics is analogous to that of the single charge-exchange (SCX) reaction, which is known to be successfully described by the eikonal diffractive model[13),14)] with the single-step process occurring on the nucleon. Since this model is simple and accurate enough for our approach, we also use it to describe the DCX reaction.

In the eikonal distorted wave approximation, the amplitude of a single-step process in a nucleus can be written as

$$F_{fi}(\vec{q}) = \frac{i k_\pi}{2\pi} \int d^2b\ e^{i\vec{q}\vec{b}} \langle \psi_f | \sum_i \Gamma_i^{DCX}(\vec{b} - \vec{S}_i) | \psi_i \rangle\ e^{i\chi_{opt}(\vec{b})} \qquad (4)$$

Here k_π is the absolute value of the incident pion momentum, $\vec{b}$ is the impact parameter, $\vec{s}_i$ is the co-ordinate of the i^{th} Δ_{33} component inside the nucleus. Further, the phase function $\chi_{opt}(\vec{b})$ is defined as

$$\chi_{opt}(\vec{b}) = -\frac{1}{\hbar v}\int_{-\infty}^{+\infty} V_{opt}(\vec{b},z)\,dz$$

$$\simeq \frac{2\pi A}{k} f_{\pi N}(0)\int_{-\infty}^{+\infty} \rho_N(\vec{b},z)\,dz \qquad (5)$$

Here, V_{opt} is the pion-nucleus optical potential, $f_{\pi N}(0)$ is the forward πN scattering amplitude, $\rho_N(\vec{b},z)$ is the single nucleon density in the nucleus, normalized so that $\int d^3\vec{r}\ \rho_N(\vec{r}) = 1$.

The so-called profile function Γ_i^{DCX} is defined as

$$\Gamma_i^{DCX}(\vec{b}) = \frac{1}{2\pi i k}\int d^2q\, e^{-i\vec{q}\cdot\vec{b}} f_{\pi\Delta}(\vec{q})\left(C^+_{\Delta^{++}} C_{\Delta^0} + C^+_{\Delta^+} C_{\Delta^-}\right) \qquad (6)$$

with $f_{\pi\Delta}(\vec{q})$ the amplitude of the double charge-exchange $\pi\Delta$ reaction and c and c^+, respectively, the corresponding annihilation and creation operators of Δ_{33}. The linear combination in the parentheses of the right-hand side of Eq. (6) takes into account the interference effect between two different channels.

Introducing the short-range approximation, we get from Eq. (6)

$$\Gamma_i^{DCX}(\vec{b}) = f_{\pi\Delta}^{DCX}(0)\,\delta(\vec{b})\left(C^+_{\Delta^{++}} C_{\Delta^0} + C^+_{\Delta^+} C_{\Delta^-}\right)\frac{2\pi}{i k_\pi} \qquad (7)$$

The transition matrix element in Eq. (4) can now be written as

$$F_{fi}(\vec{q}) = A\,\eta_\Delta\, f_{\pi\Delta}^{DCX}(0)\int d\vec{b}\ \rho_N(\vec{b})\, e^{i\vec{q}\cdot\vec{b}}\, e^{i\chi_{opt}(\vec{b})}$$

$$\left(C^{I_i\,I_i}_{\frac{3}{2}-\frac{3}{2};\,I'\,I_i+\frac{3}{2}}\ C^{I_f\,I_i+2}_{\frac{3}{2}\frac{1}{2};\,I'\,I_i+2-\frac{1}{2}} + C^{I_i\,I_i}_{\frac{3}{2}-\frac{1}{2};\,I'\,I_i+\frac{1}{2}}\ C^{I_f\,I_i+2}_{\frac{3}{2}\frac{3}{2};\,I'\,I_i+2-\frac{3}{2}}\right) \qquad (8)$$

where $C^{IM}_{I_1M_1;I_2M_2}$ is the Clebsch-Gordan coefficient, and I' is the isospin of the nuclear system with one of the Δ's removed. (For self-conjugate nuclei, $I_i = 0$,

so $I' = 3/2$ and $I_f = 2$.) We denote by η_Δ the fraction of Δ_{33} isobars (including all charge states) per nucleon, i.e., $A\eta_\Delta \equiv n_\Delta$ is the total number of Δ_{33} isobars in the nucleus. The two-dimensional single nucleon density $\rho_N(\vec{b})$ is defined as

$$\rho_N(\vec{b}) = \int_{-\infty}^{+\infty} \rho_N(\vec{b}, z)\, dz \ . \tag{9}$$

In deriving Eq. (8), we have assumed that the initial and the final wave functions of the nucleus, in which the Δ_{33} component appears as a result of fluctuations, have essentially the same structure.

An elementary consideration shows that both ρ_N and χ_{opt} must be functions of $|\vec{b}|$, so that the integration over angle in Eq. (8) can be carried out. This yields:

$$F_{fi}(\vec{q}) = \frac{2\pi A \eta_\Delta}{\sqrt{2}} f^{DCX}_{\pi\Delta}(0) \int b\, db\, J_0(qb)\, \rho_N(b)\, e^{i\chi_{opt}(b)} \ , \tag{10}$$

where J_0 is the zeroth order Bessel function.

Now, under the strong absorption assumption, $\exp(i\chi_{opt}(b))$ in Eq. (10) is close to zero for nearly all trajectories which intersect the nucleus while $\exp(i\chi_{opt}(b))$ is unity for those which completely miss the nucleus. At the same time, $\rho_N(b)$ is nearly a constant inside the nucleus dropping very rapidly to zero outside. Therefore the product of $\rho_N(b)$ and $\exp(i\chi_{opt}(b))$ gives rise to a sharp peak near the effective radius $\bar{R}$, as shown by Johnson and Bethe[15], so that the contribution of the integral in Eq. (10) comes from a narrow interval of impact parameters near $\bar{R}$, defined as

$$\left| e^{i\chi_{opt}(\bar{R})} \right| \equiv \frac{1}{2} \ . \tag{11}$$

The integrand of Eq. (10) can be roughly estimated in terms of $\bar{R}$ and a, as

$$\bar{R}\ J_0(q\bar{R})\, \rho_N(\bar{R})\, \frac{1}{2} \cdot 2a$$

where a is the so-called diffuseness parameter characterizing the thickness of nuclear surface. It follows that

$$F_{fi}(\vec{q}) = \frac{i\,2\pi a}{\sqrt{2}} f^{DCX}_{\pi\Delta}(0)\, A\eta_\Delta\, \bar{R}\, J_0(q\bar{R})\, \rho_N(\bar{R}) \ . \tag{12}$$

From the analysis given in Refs. 13) and 15) the dependence of the diffuseness parameter a on energy is weak and usually one can take a ≃ 0.6 fm.

The differential cross-section for DCX is obtained from Eq. (12) directly as

$$\frac{d\sigma}{d\Omega} \simeq \left| f_{\pi\Delta}^{DCX}(0) \right|^2 \frac{(2\pi)^2 a^2}{2} (A\eta_\Delta)^2 \bar{R}^2 \rho_N^2(\bar{R}) J_0^2(q\bar{R}) . \tag{13}$$

The effective radius $\bar{R}$ varies approximately as

$$\bar{R} \simeq r_0 A^{1/3} ,$$

where r_0 is taken as a free parameter. We later show that experiments give $r_0 \sim 1.3$ fm. Then we have

$$\frac{d\sigma}{d\Omega} = g_2^\Delta(T_\pi) J_0^2(q\bar{R}) A^{-4/3} \tag{14}$$

and

$$g_2^\Delta(T_\pi) = \left. \frac{d\sigma_{\pi\Delta}^{DCX}}{d\Omega} \right|_{0^\circ} (A\eta_\Delta)^2 \frac{(2\pi)^2 a^2 r_0^2}{2} \rho^2(\bar{R}) , \tag{15}$$

where T_π is the kinetic energy of the incident pion, $\rho(\vec{r}) \equiv A\rho_N(\vec{r})$ and $(d\sigma_{\pi\Delta}^{DCX}/d\Omega)|_{0^\circ}$ is the forward cross-section for reaction $\pi^+\Delta^- \to \pi^-\Delta^+$.

The theoretical expression given in Eqs. (14) and (15) can be directly compared with experiments. But, before doing this, we must know the forward differential cross-section $(d\sigma_{\Delta\pi}^{DEX}/d\Omega)|_{0^\circ}$. This point is discussed in the next section.

3. - THE ELEMENTARY DCX CROSS-SECTION $\pi^-\Delta \to \pi^+\Delta$

The $\pi\Delta$ elastic cross-section is not experimentally known, since both π and Δ are unstable objects. However, in the threshold region, the S-wave amplitude follows from chiral symmetry arguments using current algebra techniques. In the chiral limit the S-wave DCX amplitude vanishes exactly. At higher energies as

used here, the DCX amplitude of the $\pi\Delta$ reaction is estimated from the pole contributions of the Feynman diagrams depicted in Fig. 1. The dominant contribution comes from $\Delta(1232;\frac{3}{2}^+)$, $N^*(1440;\frac{1}{2}^+)$ and $N^*(1520;\frac{3}{2}^-)$ poles, while the nucleon $N(938;\frac{1}{2}^+)$ pole is unimportant. The coupling constants $g_{N\Delta\pi}$, $g_{N^*\Delta\pi}$,..., are experimentally known, apart from $g_{\Delta\Delta\pi}$, which we estimated by the quark model to be $(g^2_{\Delta\Delta\pi}/4\pi) \simeq 9.3$. In particular the $N^*(1520;\frac{3}{2}^-)$ gives rise to an S-wave $\pi\Delta$ resonance, which occurs at a pion kinetic energy close to that of the Δ_{33} resonance in the πN system. As for the $N^*(1440;\frac{1}{2}^+)$, it contributes to P-wave $\pi\Delta$ scattering, but its contribution is suppressed by a barrier-penetrating factor k_π^4 in the low energy region, where k_π is the pion momentum. The effective width of the excitation curve is, however, increased by this contribution.

With this theoretical $\pi\Delta \to \pi\Delta$ amplitude, Fig. 2 gives rise to the theoretical excitation curve of the forward DCX $\pi\Delta$ process in the centre-of-mass system as a function of the incident pion energy. Figure 3 gives the total charge-exchange cross-section.

4. - COMPARISON WITH EXPERIMENTS

There exists a systematic experimental study of DCX reaction on I = 0 nuclei for five incident pion energies in the region 120 MeV $\leq T_\pi \leq$ 210 MeV for the following nuclei[2),3)] ^{12}C, ^{16}O, ^{24}Mg, ^{28}Si, ^{32}S and ^{40}Ca. Furthermore, both the DIAT (double isobaric analogue transition) and non-DIAT in $^{56}Fe(\pi^+,\pi^-)^{56}Ni$ have been studied in Ref. 19) for incident pion energies of 140 MeV to 290 MeV. The energy dependence of the angular distributions at $\theta = 5°$ in the non-DIAT reaction $^{16}O(\pi^+,\pi^-)^{16}Ne$(g.s.) has been reported as well[20),21)].

From all these experimental results, one observes the following regularities of non-analogue reactions in the forward direction: (a) relatively large cross-sections compared with the analogue ones; (b) an $A^{-4/3}$ mass dependence in contrast with the $A^{-10/3}$ one for the analogue reactions; (c) excitation functions peaked near the Δ_{33} resonance at $T_\pi \approx 164$ MeV; and (d) a diffractive angular distribution near the forward direction. In short, all these features contrast with the ones observed in the analogue DCX transitions. According to Eqs. (13) and (14), the DCX differential cross-section has the following structure in the eikonal model:

$$\frac{d\sigma}{d\Omega} = \text{const.}\ (A\eta_\Delta)^2\ A^{-\frac{4}{3}}\ J_0^2(q\bar{R})\ \frac{d\sigma_{\pi\Delta}^{DCX}}{d\Omega}\Big|_{0^\circ}$$

Its characteristic factors are the following: (1) the elementary forward differential cross-section $(d\sigma_{\pi\Delta}^{DCX}/d\Omega)\big|_{0^\circ}$ gives the resonance peak at $T_\pi \tilde{=} 164$ MeV, which originates in the S-wave $\pi\Delta$ resonance at $N^*(1520;\frac{3}{2}^-)$ simulating the Δ resonance in the πN system; (2) the $J_0^2(q\bar{R})$ factor produces a diffractive structure near the forward direction; and (3) the factor $A^{-4/3}$ gives the mass dependence of the cross-section.

While the eikonal factor $A^{-4/3}$ may explain the experimental mass dependence, an important assumption must be made: the total number of Δ_{33} isobars in the nucleus, $n_\Delta \equiv A\eta_\Delta$, must be approximately constant, independent of the mass number A. We shall discuss this problem in more detail later in Section 6.

Figure 4 gives the DCX cross-sections versus A at $\theta = 5°$ for different pion energies[12]. The $^{56}Fe(\pi^+,\pi^-)^{56}Ni(g.s.)$ cross-section at $\theta = 5°$ also satisfies the $A^{-4/3}$ dependence[19] but is not shown in Fig. 4.

One finds that the $A^{-4/3}$ law holds well for all the I = 0 nuclei except for ^{24}Mg at $T_\pi = 140$ MeV. Thus Eq. (14) accounts well for this behaviour provided $n_\Delta = \text{const.}$

Figures 5 and 6 show the angular distributions for $^{12}C(\pi^+,\pi^-)^{12}O(g.s.)$ and $^{40}Ca(\pi^+,\pi^-)^{40}Ti$ at $T_\pi = 164$ MeV and for $^{16}O(\pi^+,\pi^-)^{16}Ne(g.s.)$ at $T_\pi = 164$ MeV, $T_\pi = 120$ MeV and $T_\pi = 200$ MeV. The solid curves are calculated from Eq. (13). The general trends in the angular distributions, and in particular the position of the first minimum are well reproduced by the simple function $J_0^2(q\bar{R})$, in Eq. (13) with $r_0 = 1.3$ fm as the only adjustable parameter. Beyond the first minimum, the experimental data are notably below the $J_0^2(q\bar{R})$ curves. This, however, is not surprising, since the eikonal diffractive calculation within our approximations ceases to be valid at large angles. The value $r_0 = 1.3$ fm is the same as the one determined from the SCX eikonal model[13),14].

The excitation curves at $\theta = 5°$ for different nuclei are shown in Fig. 7 and Fig. 8. All these curves are taken from Ref. 2), and have there been fitted with a Breit-Wigner formula. The peak position is close to $T_\pi = 160$–170 MeV, which corresponds to the S-wave $N^*(1520)$ resonance of the $\pi\Delta$ system with a slight downward energy shift. A similar shift is well known in pion-nucleus scattering

near the Δ_{33} resonance[22),23)] as a consequence of multiple scattering effects.

The empirical adjusted width of DCX excitation curves is $\Gamma \simeq 75$ MeV. As compared to the free $N^*(1520;\frac{3}{2}^-)$ width of 100-140 MeV, this represents an important reduction. A natural explanation of the narrowing is that the dominant decay mode of the free N*(1520) is the πN (p-wave) channel with $\Gamma(N^* \to N\pi) \tilde{=}$ 50-70 MeV. In the nuclear case, the phase space of this mode is severely decreased so that the main part of the width comes from other channels with at most 10 to 15 MeV contributing from a $(N\pi)$ branch. The observed width is thus qualitatively in agreement with the model suggested here. Figure 9 gives the comparison of the excitation function calculated using the adjusted width to the excitation curve of ^{16}O. As seen, the agreement is good.

5. - THE INTERNAL CONSISTENCY OF THE SINGLE AND DOUBLE CHARGE-EXCHANGE MECHANISM

Thus, all the important features of DCX on self-conjugate nuclei near the resonance can be explained with the one-step $\pi\Delta$ mechanism. The same eikonal diffractive model is also used to describe pion-induced SCX (single charge-exchange) reactions between the isobaric analogue states (IAS)[13),14)], but with a one-step πN mechanism. It is therefore important to compare these processes so as to see if one can obtain more information about the $\pi\Delta$ mechanism.

The SCX forward IAS cross-section also follows the $A^{-4/3}$ law, and has a diffractive angular distribution. In addition, the experimental excitation curve follows approximately that of the free $\pi^- p \to \pi^\circ n$ process with a maximum near $T_\pi \tilde{=}$ 165 MeV, i.e., at the Δ_{33} resonance[22),23)].

It is not difficult to derive the SCX cross-section explicitly in the approximation corresponding to Eq. (13):

$$\frac{d\sigma^{IAS}}{d\Omega} = g_1(T_\pi)(N-Z)\, J_0^2(qR)\, A^{-4/3} \qquad (16)$$

where N and Z are the neutron and proton numbers respectively of the target nucleus, while

$$g_1(T_\pi) = \left.\frac{d\sigma_{\pi N}^{SCX}}{d\Omega}\right|_{0^\circ} (2\pi)^2 a^2 \varrho^2(\bar{R})\, r_0^2 \qquad (17)$$

Here $(d\sigma_{\pi N}^{SCX}/d\Omega)|_{0^\circ}$ is the free $\pi^- p \to \pi^\circ N$ SCX cross-section at 0°. Thus, the eikonal-diffractive model provides a unified description of these two processes. Moreover, according to our model, the ratio $g_2^\Delta(T_\pi)/g_1(T_\pi)$ is governed by the cross-section behaviour of the two elementary processes $\pi^+ + N \to \pi^\circ + p$ and $\pi^+ + \Delta \to \pi^- + \Delta$, taken in the nuclear medium. Therefore, it depends on the pion energy in a non-trivial way. The comparison of g_1 and g_2^Δ may serve as an additional test of the consistency of the model proposed here.

6. - MASS DEPENDENCE OF THE NUMBER OF Δ ISOBARS

The eikonal Δ model offers a possible explanation to all experimentally observed features in DCX on I = 0 nuclei only if the isobar number n_Δ does not change from nucleus to nucleus. Otherwise this model will fail completely.

There are two complementary ways of viewing the quantity n_Δ. On the one hand we may consider it as occurring in the short-range interaction of two nucleons as a component of their relative wave function. Such isobars have predominantly large momentum components and give a constant isobar density in nuclear matter. On the other hand, the Δ's may also have low momentum components in which case $n_\Delta \simeq$ constant could result. This possibility is in particular realized in a Δ isobar model used by Bohr and Mottelson for an estimate of the renormalization of the axial coupling constant g_A in nuclei[16]. Although it is known that the renormalization occurs also by other mechanisms, we will investigate its consequences.

We consider explicitly the Δ component in the nuclear wave function[17]

$$\psi(\text{"}N_1 N_2 \cdots\cdots N_n\text{"}) = a_0 \psi(N_1 N_2 \cdots\cdots N_n) + a_1 \psi_1(\Delta N_2 \cdots\cdots N_n) + a_2 \psi_2(\Delta_1 \Delta_2 \cdots\cdots N_n) + \cdots\cdots \qquad (18)$$

The normalization condition requires

$$\sum_{\ell=0}^{n} a_\ell^2 = 1$$

and the probability of finding the Δ per nucleon η_Δ is

$$\eta_\Delta = \sum_{\ell=1}^{n} \ell\, a_\ell^2 \tag{19}$$

The isobar density η_Δ can now be estimated using the Bohr-Mottelson model. We outline the main steps only.

Consider an effective Landau-Migdal two-body spin-isospin interaction of the type

$$(\vec{\sigma}_1 \cdot \vec{\sigma}_2)(\vec{\tau}_1 \cdot \vec{\tau}_2)\, V(r_{12})$$

operating between nucleon pairs in the nucleus, one can construct the effective response of a spin-isospin field of long wavelength by averaging $V(r_{12})$ over the nuclear volume. In the space of nucleons this effective response is proportional to the spin-isospin operator $F_{m\mu}$ defined by

$$F_{m\mu} = \sigma_m \tau_\mu \tag{20}$$

where $\vec{\sigma}$ and $\vec{\tau}$ are the nucleon spin and isospin variables. More generally, the field $F_{m\mu}$ of Eq. (20) can be considered as operating on the quark degree of freedom with

$$F_{m\mu} = \frac{3}{5} \sum_{q=1}^{3} (\sigma_q)_m (\tau_q)_\mu , \tag{21}$$

which also in this case gives a matrix element for Δ excitation. The factor of 3/5 follows from the fact that in the nucleon the spin-isospin wave function of quarks is totally symmetric with respect to interchange of any two quarks. The effective Hamiltonian acting on a single nucleon can be written as

$$H' = \kappa \alpha F$$

where κ is the coupling constant and α is the amplitude of external field, which in our case is the spin-isospin one. For a weak field α

the nuclear ground state is now given as

$$|\rangle = |0\rangle - \frac{\kappa\alpha_0}{2\hbar} \sum_a \left(\frac{e^{-i\omega_a t}}{\omega_a - \omega_a} + \frac{e^{i\omega_a t}}{\omega_a + \omega_a} \right) F_a |a\rangle \qquad (22)$$

where $F_a = \langle a|F|0\rangle$, and $\omega_a = (E_a - E_0)/h$, and "a" labels the nuclear Δ hole excitation with the energy gap $h\omega_a$ from the unperturbed state $|0\rangle$. Since a nucleon excited to a Δ requires $h\omega_a \simeq 300$ MeV, one may neglect $h\omega_\alpha$ altogether in comparison. Thus, the probability of finding the Δ is

$$\eta_\Delta \simeq \kappa^2 \alpha_0^2 \frac{32}{25} 9A \Big/ (300\,\mathrm{MeV})^2 \qquad (23)$$

where, in deriving Eq. (23), the value of the twice-reduced matrix element

$$\langle \Delta \| F \| N \rangle = \frac{24}{5}\sqrt{2}$$

is used[16].

The coupling constant κ is expected to be approximately proportional to A^{-1} [16]. Consequently, one obtains in this model

$$\eta_\Delta \propto A^{-1}$$

so that the total number of Δ in the nucleus $n_\Delta \equiv A\eta_\Delta$ is independent of A. This result follows from the long-range of the force. We thus see that the effective n_Δ behaves quite differently in models using short-range and long-range forces. In this sense, we may consider this result as a phenomenological feature. Experiments will decide whether further discussions should be concentrated on one or the other of the two extremes.

7. - RECAPITULATION

From the analysis in the present paper, we conclude the following.

1) The experimental data for double charge-exchange reactions show a very characteristic behaviour in the resonance region. The features are strongly

suggestive of a diffractive behaviour originating in an effective single-step process. This interpretation imposes itself particularly from the angular distribution but it is also consistent with the other features.

2) While the interpretation of the single-step process is still open, we have demonstrated here that the interpretation as a $\pi^-\Delta \to \pi^+\Delta$ process is a viable one and that it involves a series of non-trivial features. Such a model of course easily accounts for the single-step aspect. It will also account rather straightforwardly for the large wave function overlap in $0^+(g.s.) \to 0^+(g.s.)$ transitions with $\Delta I = 2$. Further and surprisingly the elementary $\pi\Delta$ cross-section has an S wave $\pi\Delta$ resonance due to N*(1520) excitation located such that it will mimic the location of the P wave $\pi N \to \Delta$ resonance in the nucleus. This non-trivial feature should be amenable to explicit tests of the origin of the resonance. In addition, the width of the resonance is quite reasonable, once the closed $N^* \to \pi N$ channel is eliminated.

3) The dynamics of the scattering process does not seem to cause serious problems. On the other hand, a description in terms of Δ-isobar seemingly requires a nearly constant number of Δ's, i.e., the total number of Δ's will be constant ($\approx$0.2-0.5) if uniformly distributed over a medium-weight nucleus. This conclusion is necessary in order to describe the A-dependence of the cross-section. While this is rather unexpected, one can in fact construct models with this property for low-momentum Δ components. We believe this feature to be the one that can most easily be tested independently of DCX experiments.

In our opinion, one must seriously consider the possibility that present double charge-exchange experiments of $0^+ \to 0^+$ transition provide the first clear indication of an explicit "cold" Δ component in nuclear wave functions.

ACKNOWLEDGEMENTS

We are indebted to Professor M. Ericson for many stimulating discussions.

REFERENCES

1) Ching Chengrui and Ho Tso-hsiu - Commun.Theor.Phys. 4 (1985) 51.

2) L.C. Bland et al. - Phys.Lett. 128B (1983) 157.

3) C.L. Morris et al. - Phys.Rev. C25 (1982) 3218.

4) T.S.H. Lee, D. Kurath and B. Zeidman - Phys.Rev.Lett. 39 (1977) 1307.

5) Guang-lie Li, Chu-Hsia Li and T.S.H. Lee - Phys.Lett. 99B (1981) 200.

6) Liu Xianhui, Wu Zongen, Huang Zhachui and Li Yanggao - Sci.Sin. 24 (1981) 789.

7) P.A. Seidl et al. - Phys.Rev. C30 (1984) 962.

8) Ching Chengrui, Ho Tsohsiu and Zhao Weiqin - AS-ITP-85-014 (1985), to be published in Commun.Theor.Phys.

9) M. Doi, T. Katani, H. Nishiura and E. Takasugi - Progr.Theor.Phys. 69 (1983) 602.

10) W.C. Haxton and G.J. Stephenson Jr. - in Progr. in Particle and Nuclear Physics, Vol. 12, ed. D. Wilkinson, F.R.S. (Pergamon, Oxford, 1984).

11) M.B. Johnson, E.R. Siciliano, H. Toki and A. Wirzba - Phys.Rev.Lett. 52 (1984) 593.

12) R. Gilman et al. - Phys.Rev. C32 (1985) 349.

13) M.B. Johnson - Phys.Rev. C22 (1980) 192.

14) H.C. Jiang - Private communication.

15) M.B. Johnson and M.A. Bethe - Comments on Nucl.Part.Phys. 8 (1978) 75.

16) A. Bohr and B.R. Mottelson - Phys.Lett. 100B (1981) 10.

17) A.K. Kerman and L.S. Kisslinger - Phys.Rev. 180 (1969) 1483.

18) C. Gaarde et al. - Nucl.Phys. A369 (1981) 258.

19) P.A. Seidl et al. - Phys.Rev.Lett. 50 (1983) 1106.

20) R. Gilman et al. - Phys.Rev. C29 (1983) 2395.

21) R. Gilman et al. - Phys.Rev. C30 (1984) 962.

22) U. Sennhauser et al. - Phys.Rev.Lett. 51 (1983) 1324.

23) F. Irom et al. - Phys.Rev. D28 (1983) 2565.

FIGURE CAPTIONS

Fig. 1 The Feynman diagrams used in the $\pi\Delta$ DCX reaction.

Fig. 2 The 0° differential cross-section of $\pi^+(\Delta^{o,-}, \Delta^{+,++})\pi^-$ in the centre-of-mass system against the energy of pions in the laboratory system.

Fig. 3 The total cross-section of $\pi^+(\Delta^{o,-}, \Delta^{++,+})\pi^-$ against the energy of pions in the laboratory system.

Fig. 4 The $A^{-4/3}$ dependence of the DCX forward cross-section taken from Ref. 2).

Fig. 5 Angular distribution of $^{12}C(\pi^+,\pi^-)^{12}O(g.s)$ and $^{40}Ca(\pi^+,\pi^-)^{40}Ti(g.s)$ at T_π = 164 MeV. The solid and dashed lines are functions of $J_o^2(q\bar{R})$, with $\bar{R} \equiv r_0 A^{1/3}$, r_0 = 1.3 fm [from Ref. 2)].

Fig. 6 Angular distribution of $^{16}O(\pi^+,\pi^-)^{16}Ne(g.s)$ at T_π = 120, 164, 200 MeV. The solid, dashed and dot-dashed line are curves of $J_o^2(q\bar{R})$, with $\bar{R} \equiv r_0 A^{1/3}$, r_0 = 1.3 fm [from Ref. 20)].

Figs. 7 and 8

The excitation curves of ^{12}C, ^{16}O, ^{24}Mg, ^{28}Si, ^{32}S and ^{40}Ca; with a Breit-Wigner fit as given by Ref. 2).

Fig. 9 Excitation function at θ = 5° (laboratory) for $^{16}O(\pi^+,\pi^-)^{16}Ne(g.s)$. The curve is a Breit-Wigner fit to all the data (except the 292 MeV point) with parameters T_{res} = 171 MeV and width Γ = 75 MeV given by Ref. 20). The dashed curve is the Eq. (21) normalized at the resonance peak with a quenching factor f = 0.75.

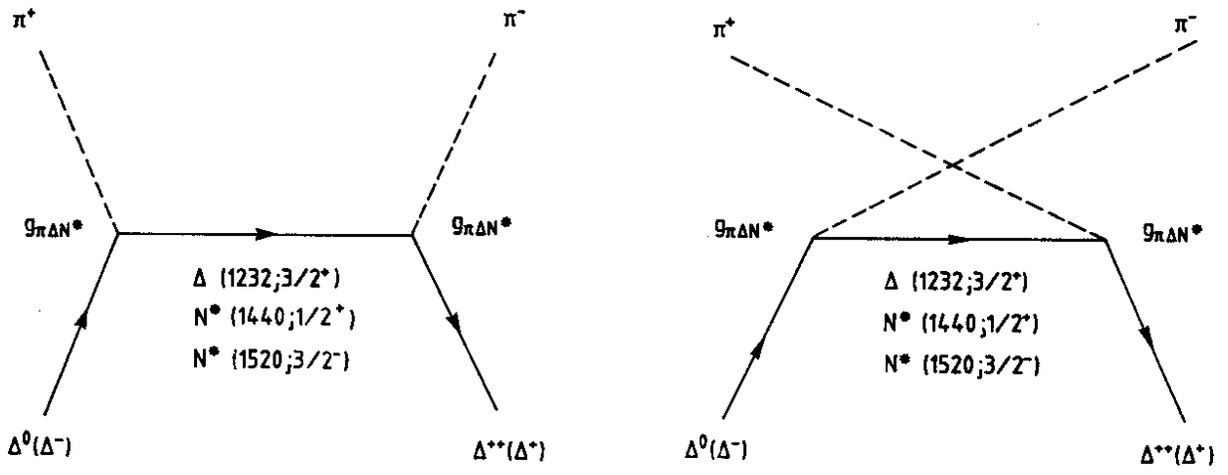

- Figure 1 -

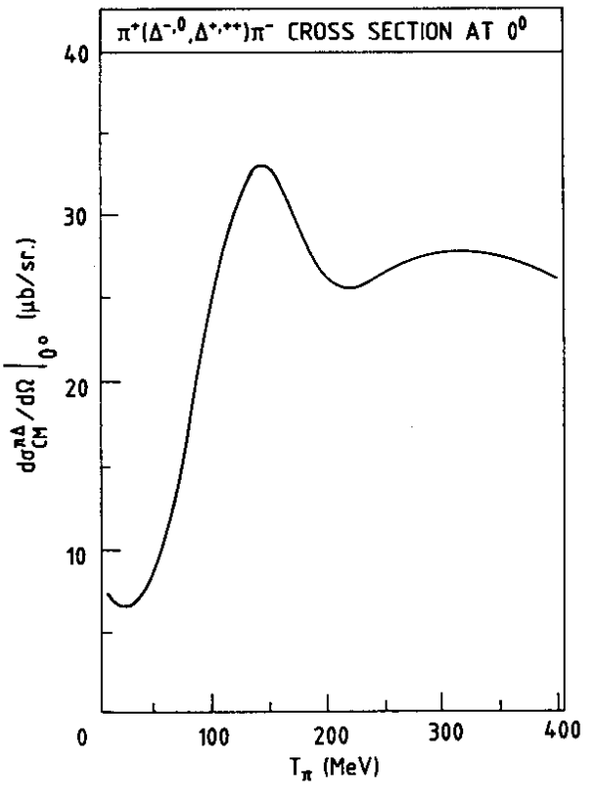

- Figure 2 -

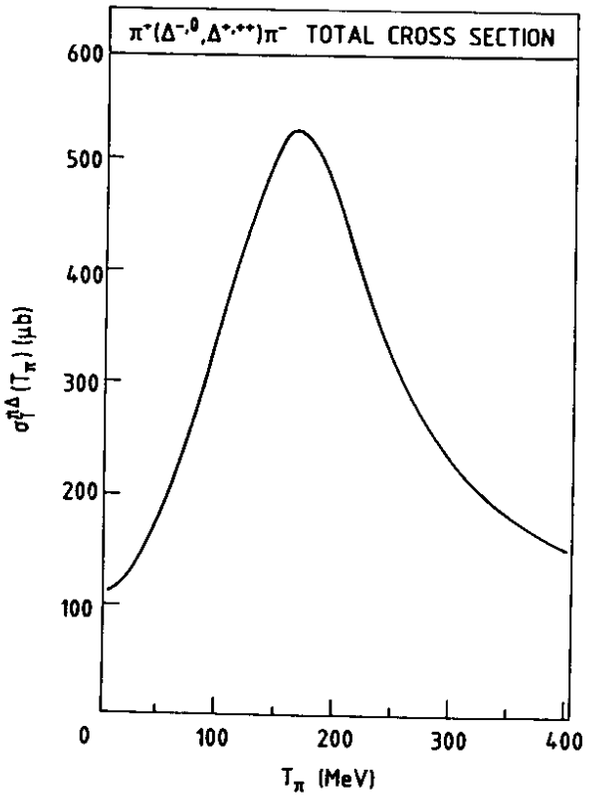

- Figure 3 -

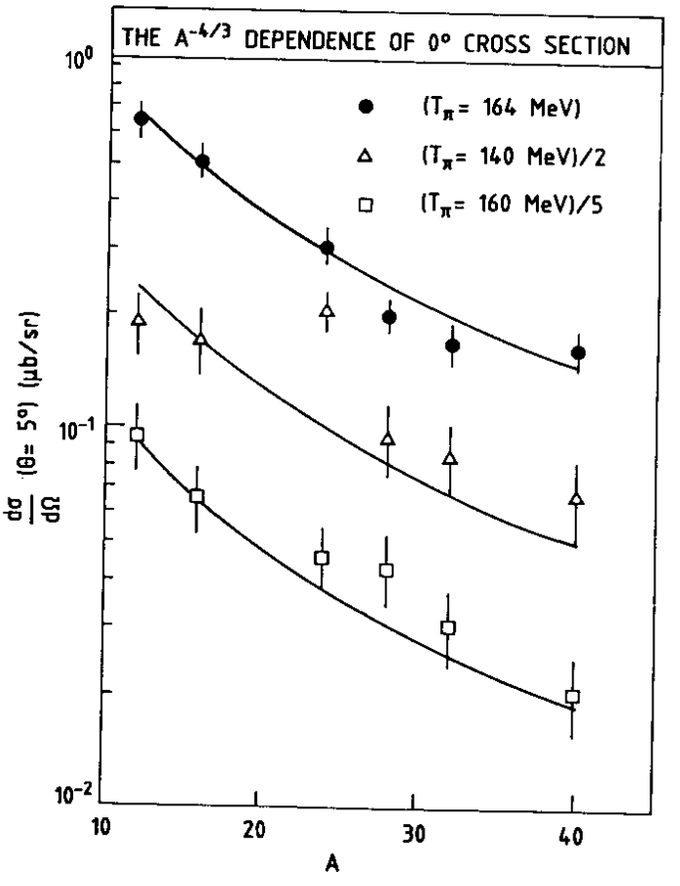

- Figure 4 -

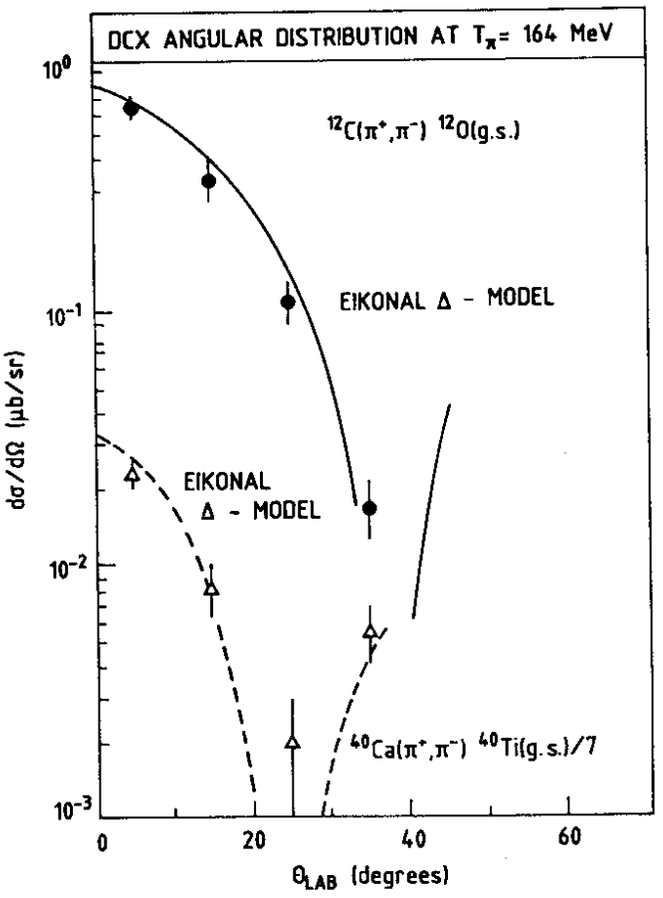

- Figure 5 -

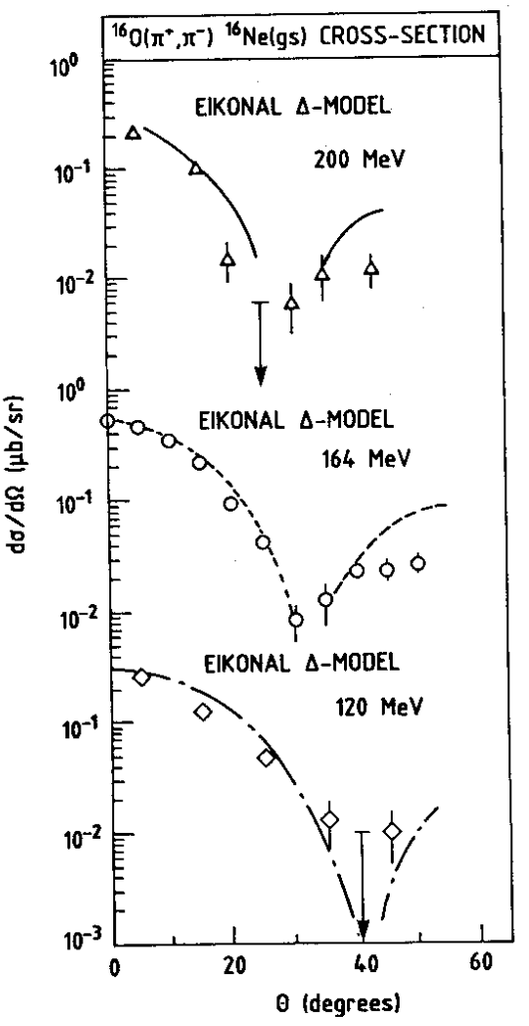

- Figure 6 -

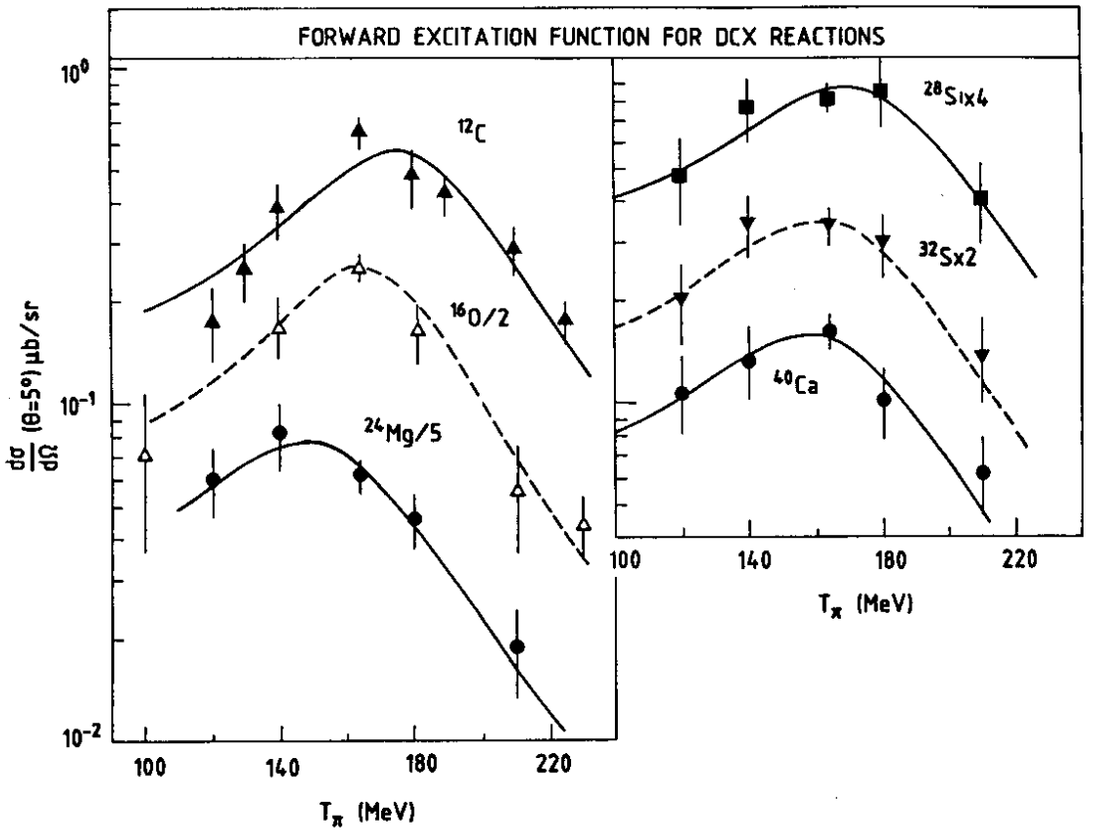

- Figure 7 -

- Figure 8 -

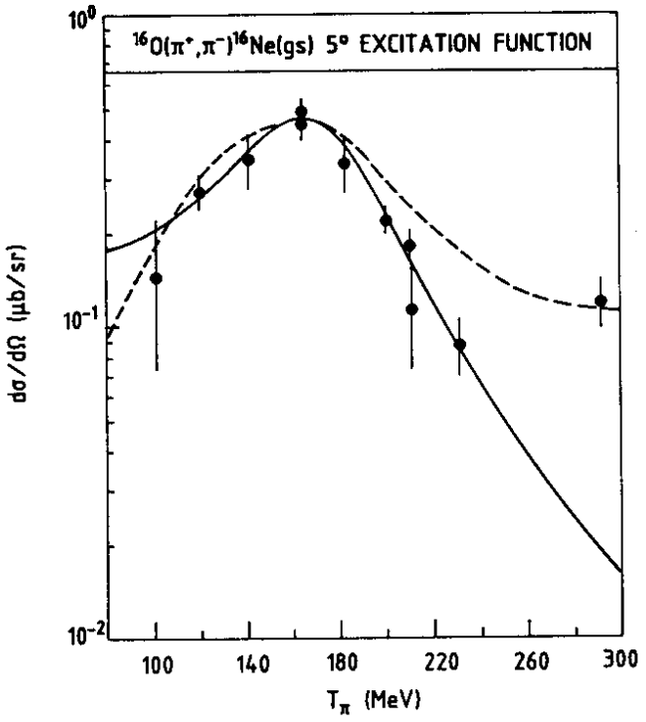
$^{16}O(\pi^+,\pi^-)^{16}Ne(gs)$ 5° EXCITATION FUNCTION
10^0
10^{-1}
10^{-2}
$d\sigma/d\Omega$ (μb/sr)
100
140
180
220
260
300
T_π (MeV)

- Figure 9 -